RSC Advances

PAPER

View Article Online
View Journal | View Issue

Check for updates

Cite this: *RSC Adv.*, 2019, **9**, 40966

Thermoresponsive P(HEMA-*co*-OEGMA) copolymers: synthesis, characteristics and solution behavior†

Maciej Kasprów, Justyna Machnik, Łukasz Otulakowski, Andrzej Dworak and Barbara Trzebicka*

Random, thermoresponsive copolymers of 2-hydroxyethyl methacrylate (HEMA) and oligo(ethylene glycol) methyl ether methacrylate M_n = 300 (OEGMA) were synthesized *via* atom transfer radical polymerization (ATRP) in a DMSO/H_2O solvent mixture. Reactivity ratios were determined by the extended Kelen–Tudos method and found to be close to 1. Studies confirmed the randomness of the obtained copolymers. The thermoresponsiveness in water and in phosphate buffer (PBS) solutions and the influence of copolymer composition and solution concentration on the cloud point temperature (T_{cp}) were investigated. Phase transitions in water solutions were reversible and narrow. The response of P(HEMA-*co*-OEGMA) to temperature could be adjusted in the range from 66.5 °C to 21.5 °C by changing the HEMA content. In PBS solutions, significant differences in the heating/cooling cycle were observed for all investigated concentrations. The presence of kosmotropic salts in PBS decreased the T_{cp} value and caused thermal aggregation of chains to form a macroscopic aggregate at temperatures above the T_{cp}.

Received 19th November 2019
Accepted 3rd December 2019

DOI: 10.1039/c9ra09668j

rsc.li/rsc-advances

Open Access Article. Published on 11 December 2019. Downloaded on 2/20/2026 5:30:21 AM.
This article is licensed under a Creative Commons Attribution-NonCommercial 3.0 Unported Licence.

Introduction

Recently, there have been many studies on polymers that are sensitive to environmental stimuli, including pH, light and temperature.[1–3] These polymers are interesting starting materials for products with controllable properties. The group of stimuli-responsive polymers includes thermoresponsive polymers showing lower critical solution temperature (LCST), *i.e.*, soluble in water only below a certain temperature, and upper critical solution temperature (UCST), *i.e.*, soluble only above a certain temperature.[4–6] The basic parameter characterizing the temperature properties of thermoresponsive polymers is the cloud point temperature (T_{cp}). The cloud point temperature of thermoresponsive polymers can be adjusted within a wide range by changing various parameters, such as the composition of the copolymers and their concentration in solution.[7,8] The group of LCST-type polymers is large. The thermoresponsive polymers that have been examined most thoroughly are poly(*N*-isopropylacrylamide) (PNIPAM),[9–11] polyoxazolines[12,13] and (co) polymers of oligoethylene glycol methacrylates (OEGMA).[7,14–16] Thermoresponsive copolymers of OEGMA have been used, for example, for the fabrication of nanocarriers[8,17,18] and as surfaces for cell proliferation and cell detachment.[19,20]

For many years, polymers based on 2-hydroxyethyl methacrylate (HEMA) have been intensively studied because of their use in medicine. The advantage of HEMA is the simplicity of its functionalization. The presence of a reactive primary hydroxyl group in the HEMA molecule allows easy modification both before and after polymerization, including the introduction of drug molecules or other reactive groups and the grafting of polymer chains.[21–28] The majority of HEMA (co)polymers, *e.g.*, with styrene, dimethyl siloxane,[29] alkyl methacrylates,[30] *N*-vinyl pyrrolidone,[31] and L-histidine,[32] have properties desirable for medical applications, such as good biocompatibility and hemocompatibility, lack of cytotoxicity and hydrophilicity.[21] These materials are used in various forms in dentistry, ophthalmology, and tissue engineering; for the production of hemodialysis membranes and implants; and for the immobilization of enzymes, cells or drugs.[21,22,29] The conjugation of HEMA (co)polymers with drugs[25–28] and the possibility of using HEMA polymers in carriers of biologically active substances[33–35] have been tested.

Despite the hydrophilic nature of the HEMA monomer, its homopolymer is, in most cases, not soluble in water. It is associated with the formation of aggregates through inter- and intrachain hydrogen bonds.[21,36–38] Hydrogen bonds can affect on PHEMA water solubility as well as on HEMA monomer reactivity in copolymerization. By selecting the appropriate solvent, it is possible to break the intermolecular hydrogen bonds which result in a decrease in HEMA reactivity or introduce competitive

Centre of Polymer and Carbon Materials, Polish Academy of Sciences, M. Curie-Skłodowskiej 34, Zabrze 41-819, Poland. E-mail: btrzebicka@cmpw-pan.edu.pl

† Electronic supplementary information (ESI) available: GPC chromatograms for different conversions, d*n*/d*c* values calculated for obtained copolymers, plots of transmittance *versus* temperature for aqueous and PBS solutions of P(HEMA-*co*-OEGMA)s, amounts of monomers used in kinetic studies, Monte Carlo simulation data. See DOI: 10.1039/c9ra09668j

This journal is © The Royal Society of Chemistry 2019

Open Access Article. Published on 11 December 2019. Downloaded on 2/20/2026 5:30:21 AM.
This article is licensed under a Creative Commons Attribution-NonCommercial 3.0 Unported Licence.

hydrogen bonds what results in increase in HEMA reactivity.[39] Choosing the right solvent for copolymerization of HEMA allows to control the distribution of units in the copolymer chain.[39,40] The impact of hydrogen bonds on the solubility of PHEMA in water was described by Weaver *et al.*[36] The authors observed that at a degree of polymerization below 30, PHEMA was soluble in water at any temperature. For degrees of polymerization in the range of 30–45, PHEMA was thermoresponsive in water. At degrees of polymerization above 45, PHEMA was insoluble in water and formed a gel. The presence of inter and intrachain hydrogen bonds limits the possibility of solvation of individual polymer chains, and for longer chains of PHEMA, these bonds lead to the formation of a water-insoluble gel. Studying the transmittance of an aqueous PHEMA solution, Longenecker *et al.*[37] showed that for PHEMA with a molar mass of 4 kDa, the hydrogen bonds break at temperatures above 80 °C, which corresponds to the UCST type transition. The occurrence of this transition and the temperature at which it appears were dependent on the polymer concentration in the aqueous solution. In the same work, the behavior of poly((2-hydroxyethyl)methacrylate-*co*-[3-(methacryloylamino)propyl]trimethylammonium chloride) and poly(2-hydroxyethyl methacrylate-*co*-[2-(methacryloyloxy)ethyl]trimethylammonium chloride) copolymers in aqueous solutions was tested. These copolymers exhibited both LCST and UCST transitions in a solution containing sodium chloride and under appropriate conditions (salt concentration, pH, ionic strength).[37]

Shen *et al.*[41] studied random copolymers of NIPAM and HEMA. The presence of HEMA in the random copolymer caused a decrease in T_{cp} compared to the T_{cp} for the PNIPAM homopolymer. It is possible to control the phase transition temperature in the range from 17 °C with a HEMA content of 35 mol% to 30.3 °C for HEMA content of 8.4 mol%. A linear dependence of T_{cp} on the HEMA content in the copolymer was observed. Fares *et al.*[42] synthesized copolymers of NIPAM and HEMA with alternating microstructures and examined their thermoresponsiveness. The observed dependence of T_{cp} on the HEMA content in the copolymer was not linear, and an increase in the HEMA up to 50% caused an increase in the phase transition temperature.

Li *et al.*[43] synthesized thermoresponsive terpolymers of HEMA, (diethylene glycol) methyl ether methacrylate and oligo(ethylene glycol) methyl ether methacrylate with M_n = 475 g mol^{-1}. They observed that an increase in the HEMA content in the terpolymer from 7 to 11 mol% led to a decrease in T_{cp} from 33 °C to 31 °C. Khutoryanskaya *et al.*[44] also found a decrease in T_{cp} for the P(HEMA-*co*-HEA) copolymers with increasing HEMA content in the chain.

HEMA is a useful monomer in conjugation due to the possibility of different kinds of its modifications. The homopolymer of HEMA soon starts to become insoluble in water with increasing molar mass and form gel. This is a serious hindrance to any possible applications.

The aim of this work was to obtain a series of water-soluble at room temperature, linear, random copolymers of 2-hydroxyethyl methacrylate (HEMA) and oligo(ethylene glycol) methyl ether methacrylate (OEGMA) with thermoresponsive properties. This work is an introduction to the research oriented toward obtaining thermoresponsive drug conjugates for potential use as carriers for controlled release of drugs. In this work, we synthesized P(HEMA-*co*-OEGMA) copolymers with controlled composition and molar mass and investigated their behavior in water and phosphate buffer (PBS). Thus far, the synthesis and solution behavior of the thermoresponsive linear polymer P(HEMA-*co*-OEGMA) have not been described. Compared to previous works, the use of controlled copolymerization of HEMA and OEGMA led to thermoresponsive copolymers with a narrow phase transition and with the possibility of controlling the transition temperature in a wide range from 21.5 °C to 66.5 °C. Higher phase transition temperatures allow the conjugation of hydrophobic molecules to the polymer chain without lowering the phase transition temperature below physiological temperature.

The reported study of P(HEMA-*co*-OEGMA), opens the route to possible applications of this copolymer in medicine. The envisaged aim is to obtain drug conjugates (*via* a covalent bond) of thermoresponsive HEMA based copolymers with phase transition close to the physiological temperature, capable of forming mesoglobules with appropriate sizes. They could, then, be stabilized for use as nanocarriers as we have described before.[45–48]

The synthesis was carried out using atom transfer radical polymerization (ATRP) in a binary DMSO/H_2O solvent system. The water solution behavior of P(HEMA-*co*-OEGMA) with various compositions was studied and compared to determine the impact of HEMA on the thermoresponsive behavior of copolymers and to determine the relationship between the composition of copolymers and the T_{cp}. The same studies were carried out in PBS to determine the influence of kosmotropic salts on the temperature response of copolymers.

Materials and methods

Materials

Ethyl 2-bromo-2-methylpropionate (EBiB, 98%), 2-hydroxyethyl methacrylate (HEMA, ≥99%), oligo(ethylene glycol) methyl ether methacrylate (OEGMA, M_n = 300 g mol^{-1}), copper(I) bromide (CuBr, 98%), benzyl alcohol (BA, ≥99%) and tris[2-(dimethylamino)ethyl]amine (Me_6TREN, ≥99%) were purchased from Sigma-Aldrich. HEMA and OEGMA were purified by passing over a short column of activated basic alumina (Sigma-Aldrich) to remove the inhibitor and stored at −27 °C. Copper bromide was purified according to methods described in ref. 49 and 50 and stored under argon at 4 °C. Dimethyl sulfoxide (DMSO, ≥99.5%, for HPLC) purchased from POCH S.A. (Gliwice, Poland) and water (HPLC Plus) purchased from Sigma-Aldrich were purged with argon before use. Concentrated phosphate-buffered saline (PBS, BioUltra) from Sigma-Aldrich was used after tenfold dilution with filtered, deionized water.

Polymerization of OEGMA and copolymerization of HEMA and OEGMA

The copolymers of HEMA and OEGMA (P(HEMA-*co*-OEGMA)) and the homopolymer of OEGMA (POEGMA) were synthesized

Open Access Article. Published on 11 December 2019. Downloaded on 2/20/2026 5:30:21 AM. This article is licensed under a Creative Commons Attribution-NonCommercial 3.0 Unported Licence.

using controlled radical polymerization. A binary solvent mixture (DMSO/H_2O; 9 : 1; v : v) was used in the synthesis. For the copolymers, the procedure was as follows. Solvents (3.58 mL DMSO and 0.4 mL of water) and CuBr (7.17 mg; 0.05 mmol) were added to a reactor fitted with a magnetic stirrer. The reactor was immersed in a water bath at 25 °C and purged with argon for 20 min. Simultaneously, to the second reactor HEMA (0.57 mL; 4.65 mmol), OEGMA (1.33 mL; 4.65 mmol), DMSO (3.58 mL), water (0.4 mL), EBiB (3.67 μL; 0.025 mmol) and BA (0.19 mL) as the standard for RP HPLC measurements were added. The mixture was purged with argon for 40 min. After 20 min of purging the first reactor, Me_6TREN (6.68 μL; 0.025 mmol) was added, and the mixture was further purged with argon for another 20 min. Then, the contents of the second reactor were poured into the first reactor. Then, the reactor was sealed. The polymerizations were carried out to approximately 50% conversion. The obtained polymers were purified by dialysis in a membrane (MWCO 6000–8000) for 2 days against water, 2 days against a water–acetone mixture and another 2 days in pure acetone. After dialysis, the solutions from the membranes were evaporated on a rotary pump, and the products were dried under vacuum. The procedure of polymerization of OEGMA (1.9 mL; 6.67 mmol) was analogous to that described for copolymers.

Methods

Nuclear magnetic resonance spectroscopy. The ^{1}H NMR spectra of (co)polymers were recorded on a Bruker Ultrashield spectrometer operating at 600 MHz using DMSO-d_6 as the solvent without using TMS as an internal standard. The DMSO-d_6 chemical shift was set to 2.49 ppm.

Gel permeation chromatography. Gel permeation chromatography (GPC) measurements of the (co)polymers were performed at 45 °C in *N*,*N*-dimethylformamide (DMF) with the addition of 5 mmol L^{-1} LiBr at a nominal flow rate of 1 mL min^{-1}. The chromatography system contained a multiangle light scattering detector (DAWN HELEOS, Wyatt Technology, λ = 658 nm), a refractive index detector (Dn-2010 RI, WGE Dr Bures), and a column system (PSS gel GRAM guard and three columns PSS GRAM 100 Å, 1000 Å and 3000 Å). The molar mass and dispersity were evaluated using ASTRA 5.3.4.10 software from Wyatt Technologies. The refractive index increments (dn/dc) of the copolymers were calculated based on the equation:[51]

$$\left(\frac{dn}{dc}\right) = \left(\frac{dn}{dc}\right)_1 w + \left(\frac{dn}{dc}\right)_2 (1 - w)$$

where: $\left(\frac{dn}{dc}\right)_1$ is the value for the homopolymer of monomer 1, $\left(\frac{dn}{dc}\right)_2$ is the value for the homopolymer of monomer 2, w is the mole fraction of monomer 1 in copolymer.

Reversed-phase high-performance liquid chromatography. RP HPLC was applied to determine the conversion of monomers during polymerization. One-microliter samples were collected at specified times during polymerization. Each sample was diluted a thousand times in a water and acetonitrile mixture (7 : 3, v : v) and then six times in water. The solvents used had 0.1 wt% trifluoroacetic acid (TFA). An Agilent 1260 Infinity system with an Agilent 1260 DAD VL UV-Vis diode array detector was equipped with an Agilent ZORBAX Eclipse XDB C18 4.6 × 150 mm column. A linear gradient from 10% to 95% acetonitrile with 0.1 wt% TFA over 30 min and a flow rate of 0.5 mL min^{-1} were applied. The lessening of monomers was monitored at 210 nm. Chromatograms were recorded using the Agilent ChemStation software.

Turbidimetry. The cloud point temperatures of the copolymers in solution were determined using a SPECORD 200 PLUS UV-Vis spectrophotometer from Analytik Jena with a Peltier temperature-controlled cell holder. The transmittance of the copolymer solutions in water and in PBS at concentrations of 0.25 g L^{-1}, 0.5 g L^{-1} and 1 g L^{-1} as a function of temperature were monitored during heating and cooling at a wavelength of λ = 500 nm. Solutions were heated gradually with a 1 °C step to the final temperature with a precision of 0.5 °C. The stabilization time after reaching the temperature was 120 s.

Results

The P(HEMA-*co*-OEGMA) copolymers and P(OEGMA) homopolymer were synthesized using atom transfer radical polymerization (ATRP).[52,53] A schematic representation of the copolymer synthesis is shown in Scheme 1. Teoh *et al.*[40] demonstrated that the use of DMSO as a solvent in the copolymerization of HEMA and DMAEMA by ATRP leads to a random distribution of the units in the chains of their copolymers. In this article, to carry out the copolymerization of HEMA and OEGMA, the DMSO/water system (9 : 1, v : v) was used, assuming that DMSO would promote the generation of random copolymer chains. The addition of water in the reaction system was aimed at accelerating the reaction due to the much greater disproportionation constant of copper bromide in water than in pure DMSO.[54]

The HEMA content in the reaction mixture was varied from 30 to 90 mol%. The resulting copolymers are described further using the designation P(HEMA$_{(x)}$-*co*-OEGMA$_{(100-x)}$), where x is mol% of HEMA in the copolymer chain.

The composition of the obtained copolymers was calculated based on their ^{1}H NMR spectra in d_6-DMSO. An exemplary ^{1}H NMR spectrum of P(HEMA$_{70}$-*co*-OEGMA$_{30}$) is shown in Fig. 1.

In the spectrum, a signal at a chemical shift of 3.26 ppm is present, which is attributed to the three protons of the methoxy group from the OEGMA side chain (5), and a signal at a chemical shift of 4.75 ppm, which is attributed to the one proton of

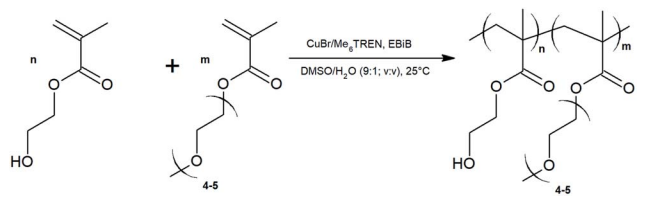

Scheme 1 Schematic representation of the polymerization reaction of HEMA and OEGMA by controlled radical polymerization.

Open Access Article. Published on 11 December 2019. Downloaded on 2/20/2026 5:30:21 AM. This article is licensed under a Creative Commons Attribution-NonCommercial 3.0 Unported Licence.

the hydroxyl group in the HEMA side chain (8). The signals at a chemical shift of 3.26 together with the signal at a shift of 3.90–4.01 ppm, which is attributed to the four protons of the methylene group (3 and 6) in the side chain of HEMA and OEGMA, allow calculating the P(HEMA-*co*-OEGMA) composition. The composition of the copolymers was calculated based on the integration of these signals (a_5 and $a_{3,6}$) using the following formula:

$$\%\ \text{mol HEMA} = \frac{\left(\frac{\left(a_{3,6} - \left(2\left(\frac{a_5}{3}\right)\right)\right)}{2}\right)}{\left(\frac{\left(a_{3,6} - \left(2\left(\frac{a_5}{3}\right)\right)\right)}{2}\right) + \left(\frac{a_5}{3}\right)} \times 100\%$$

Table 1 shows the amount of HEMA used in the copolymerization reaction of HEMA and OEGMA and the compositions of the copolymers calculated from the ^{1}H NMR spectra. The calculated compositions of the copolymers were similar to the initial composition of the reaction mixture in all cases.

The molar mass and molar mass distributions of the obtained copolymers were determined using GPC-MALS measurements. The chromatograms of all copolymers were monomodal. The exemplary chromatograms of P($HEMA_{70}$-*co*-$OEGMA_{30}$), P($HEMA_{80}$-*co*-$OEGMA_{20}$) and P($HEMA_{40}$-*co*-$OEGMA_{60}$) are shown in Fig. 2. The chromatograms for subsequent conversions of P($HEMA_{50}$-*co*-$OEGMA_{50}$) are presented in Fig. S1.† The refractive index increment (dn/dc) of copolymers in DMF was calculated as in ref. 51 for previously determined copolymer composition using dn/dc for PHEMA taken from ref. 55 and dn/dc for $POEGMA_{300}$ from ref. 15. The calculated dn/dc values for P(HEMA-*co*-OEGMA) copolymers with different compositions and for HEMA and OEGMA homopolymers are shown in Table S1.† The number average molar mass of the copolymers ranged from 33 kDa to 66 kDa, and the values of M_w/M_n did not exceed 1.45 (Table 1).

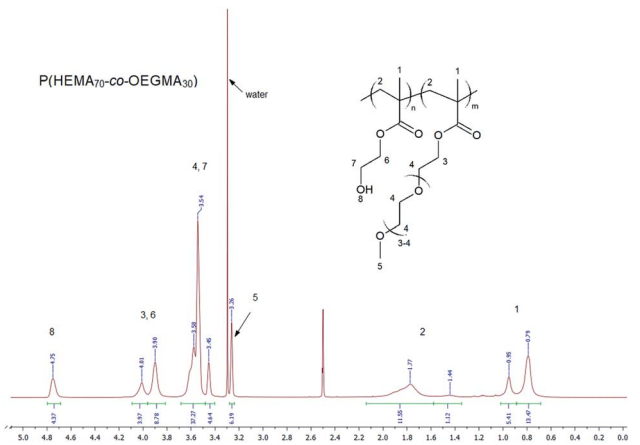

Fig. 1 ^{1}H NMR (600 MHz) spectra of P($HEMA_{70}$-*co*-$OEGMA_{30}$) in d_6-DMSO.

Polymerization kinetics of HEMA and OEGMA

The polymerization kinetics were determined for HEMA and OEGMA mixtures containing 90 mol%, 80 mol%, 50 mol%, 30 mol% and 10 mol% of HEMA (Table S2†). Samples from the reaction mixture were collected at predetermined time intervals. Monomer conversion was determined from RP HPLC chromatograms. The kinetic data for the copolymerization in the HEMA/OEGMA system with the 50% HEMA content in the feed are shown in Fig. 3.

The consumption of both monomers during the reaction was uniform for all systems, indicating similar values of the reactivity ratios of the used comonomers.

The plot of ln([M]$_0$/[M]) *versus* time shows a distinct nonlinearity. The reaction order was determined on the basis of kinetic data for the HEMA/OEGMA polymerization system and the 50% HEMA content in the feed. The course of the function in Fig. 3 indicates that the HEMA/OEGMA copolymerization do not follow classical first-order kinetics. A good fit of experimental data was obtained using the $t^{2/3}$ Fisher model (eqn (1)).[56]

$$\ln\left(\frac{[M]_0}{[M]}\right) = \frac{3}{2}k_p([RX]_0[Cu(I)]_0)^{\frac{1}{3}}\left(\frac{K_{eq}}{3k_t}\right)^{\frac{1}{3}}t^{\frac{2}{3}} \quad (1)$$

[M]$_0$ – initial monomer concentration, [M] – monomer concentration at a given time, k_p – propagation rate constant, [RX]$_0$ – initial initiator concentration, [Cu(I)]$_0$ – initial concentration of CuBr, k_t – termination rate constant, K_{eq} – equilibrium constant, t – time.

The obtained dependence $\ln([M]_0/[M_t]) = f(t^{2/3})$ was linear and had a good fit, which means that the obtained data were consistent with the $t^{2/3}$ Fischer model for homogeneous systems (Fig. 4). This indicates that the termination of the growing chains cannot be neglected. Such behavior corresponds to the kinetics of 1/3-order to the initiator.

To determine the microstructure of the obtained copolymers, the monomer reactivity ratios r_{HEMA} and r_{OEGMA} in the reaction system were calculated using the extended Kelen–Tudos method.[57] This method is usually used to determine the reactivity ratios for kinetic data obtained at high conversions above 20%. To determine the reactivity ratios, the kinetic data for samples taken from the reaction mixture after one hour from the start of polymerization were taken into account. Kinetic measurements for HEMA/OEGMA systems with different initial compositions were performed. The obtained kinetic data were subjected to transformations to draw the linear relationship presented in Fig. 5. The coefficients ξ and η present in Fig. 5 were calculated based on the formulas given in ref. 58.

The reactivity ratios for both monomers were calculated based on the $\eta = f(\xi)$ dependence from Fig. 5. The reactivity ratios had similar values of $r_{HEMA} = 0.95$ and $r_{OEGMA} = 1.18$. It follows that OEGMA in the used reaction system is slightly more reactive than HEMA and that the distribution of the units in the polymer chain is practically random. Monte Carlo simulations based on calculated reactivity ratios show the random microstructure of the P(HEMA-*co*-OEGMA) chain (Fig. S2†).

Open Access Article. Published on 11 December 2019. Downloaded on 2/20/2026 5:30:21 AM. This article is licensed under a Creative Commons Attribution-NonCommercial 3.0 Unported Licence.

Table 1 Characteristics of the obtained copolymers

	Content in feed	Content in (co)polymer			
Polymer	HEMA [mol%]	HEMA[a] [mol%]	OEGMA[a] [mol%]	M_n[b] [kDa]	M_w/M_n[b]
POEGMA	—	—	100	45	1.40
P(HEMA$_{30}$-*co*-OEGMA$_{70}$)	30	30.5	69.5	59	1.41
P(HEMA$_{40}$-*co*-OEGMA$_{60}$)	40	37.5	62.5	33	1.44
P(HEMA$_{50}$-*co*-OEGMA$_{50}$)	50	48.1	51.9	42	1.21
P(HEMA$_{60}$-*co*-OEGMA$_{40}$)	60	61	39	48	1.25
P(HEMA$_{70}$-*co*-OEGMA$_{30}$)	70	67.7	32.3	44	1.2
P(HEMA$_{80}$-*co*-OEGMA$_{20}$)	80	79.7	20.3	33	1.2
P(HEMA$_{90}$-*co*-OEGMA$_{10}$)	90	90.1	9.9	66	1.45

[a] Obtained from ^{1}H NMR spectra. [b] Obtained from GPC after dialysis.

The results discussed above show that the solvent system and the selected catalytic system used allows control of the copolymerization reactions of HEMA and OEGMA.

P(HEMA-*co*-OEGMA)s behavior in water solution

The behavior of the copolymers as a function of temperature was tested in aqueous solutions by monitoring their transmittance of UV-Vis light. Copolymer solutions with concentrations from 0.25 g L^{-1} to 1 g L^{-1} were examined. All synthesized P(HEMA-*co*-OEGMA) copolymers showed thermoresponsive behavior. For copolymer solutions with a concentration of 1 g L^{-1}, the phase transitions were sharp (3–5 °C range). The values of the cloud point temperatures were determined from the transmittance measurements assuming T_{cp} to be the temperature value at a point of 50% decrease of transmittance during the heating cycle. Exemplary dependences of transmittance as a function of temperature for two selected copolymers, P(HEMA$_{70}$-*co*-OEGMA$_{30}$) and P(HEMA$_{30}$-*co*-OEGMA$_{70}$), are shown in Fig. 6a. The dependence of transmittance on temperature for the remaining copolymers is shown in Fig. S3.† For all copolymers, a decrease in the concentration of the solution causes the shift of T_{cp} towards higher temperatures and the increase in the width of transition (Fig. 6b).

For all aqueous copolymer solutions, regardless of their composition and solution concentration, no hysteresis was observed during the heating and cooling cycles.

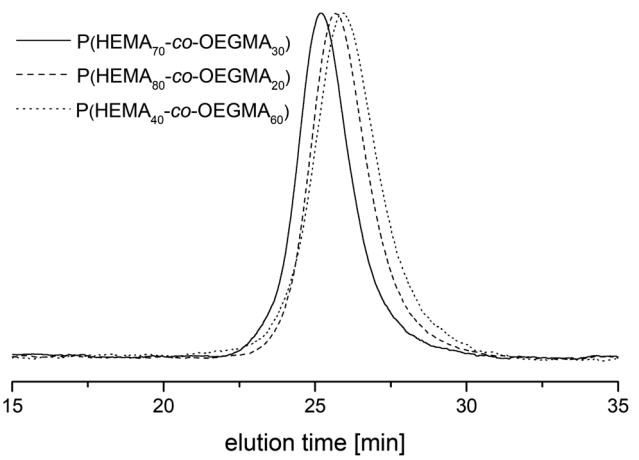

Fig. 2 The GPC chromatograms of P(HEMA$_{70}$-*co*-OEGMA$_{30}$) (straight line), P(HEMA$_{80}$-*co*-OEGMA$_{20}$) (dash) and P(HEMA$_{40}$-*co*-OEGMA$_{60}$) (dot).

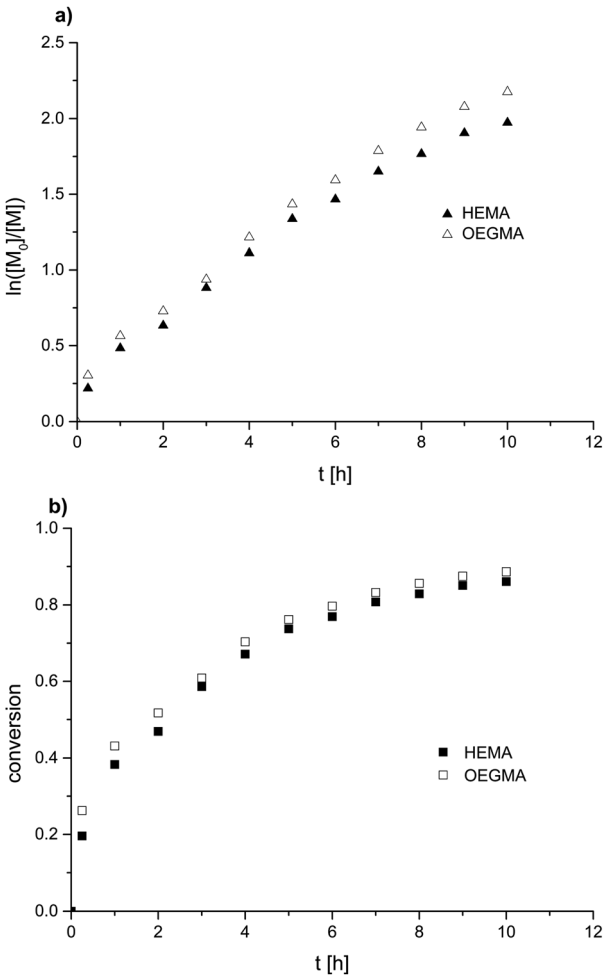

Fig. 3 (a) Kinetic plot and (b) conversion data for the synthesis of P(HEMA$_{50}$-*co*-OEGMA$_{50}$).

 This journal is © The Royal Society of Chemistry 2019

Open Access Article. Published on 11 December 2019. Downloaded on 2/20/2026 5:30:21 AM.
This article is licensed under a Creative Commons Attribution-NonCommercial 3.0 Unported Licence.

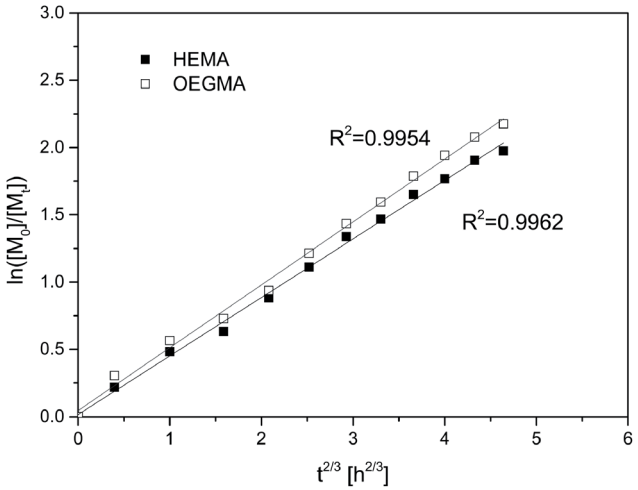

Fig. 4 Matching kinetic data for HEMA/OEGMA polymerization with 50 mol% of HEMA to the $t^{2/3}$ Fischer's model.

The effect of the copolymer composition on the T_{cp} value at different solution concentrations is shown in Fig. 7. The transition temperature decreased with increasing HEMA content in the copolymer in a nonlinear manner, following the logarithmic function with formula $y = a\ln(-b\ln(x))$. The T_{cp} of copolymers was more sensitive to copolymer composition when the content of HEMA in the polymer chain increased above 50 mol%.

The T_{cp} values for all copolymers and OEGMA homopolymer with $M_n = 45$ kDa are presented in Table S3.†

The shift of the turbidity temperatures towards lower values with the increase in the content of HEMA units shows that the HEMA units in the copolymer act as hydrophobic fragments, as intermolecular and intramolecular HB between HEMA units in the polymer chains, competes with the interaction with water molecules.[36–38,59] A similar influence of HEMA units on the T_{cp} of the copolymer was noted by Shen *et al.*[41] for the thermoresponsive copolymer P(NIPAM-*co*-HEMA). The impact of hydrogen bonds on a thermal aggregation of polymer chains could be also observed in case of copolymers of OEGMA and monomers with free oxime group.[60,61] By changing the composition of P(HEMA-*co*-OEGMA) and its concentration in solution, it is possible to control the temperature of the phase transition in the range from 21.5 °C to 66.5 °C.

It should be emphasized that even the copolymer P($HEMA_{90}$-*co*-$OEGMA_{10}$) with a number average molar mass of 66 kDa and of HEMA content of 90 mol% was completely soluble in water at temperatures slightly below 20 °C. Its phase transition was fully reversible. The presence of only 10 mol% of OEGMA in the chain caused the copolymer to behave quite differently from the insoluble HEMA homopolymer.[36,59]

The dependence of T_{cp} on the composition shown in Fig. 7 indicates that for all copolymer compositions T_{cp} slightly increases with increasing solution concentration. The logarithmic correlation between T_{cp} and the composition of the copolymer did not change with concentration but shifted slightly along the y axis, as shown in Fig. 7. The significant effect

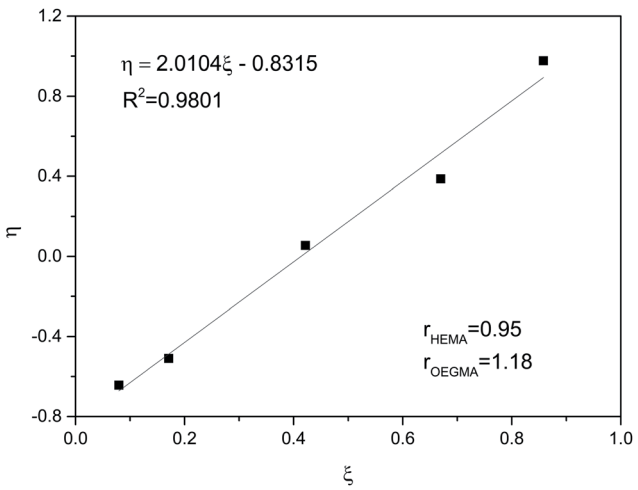

Fig. 5 Determination of reactivity ratios of monomers by the extended Kelen–Tudos method.

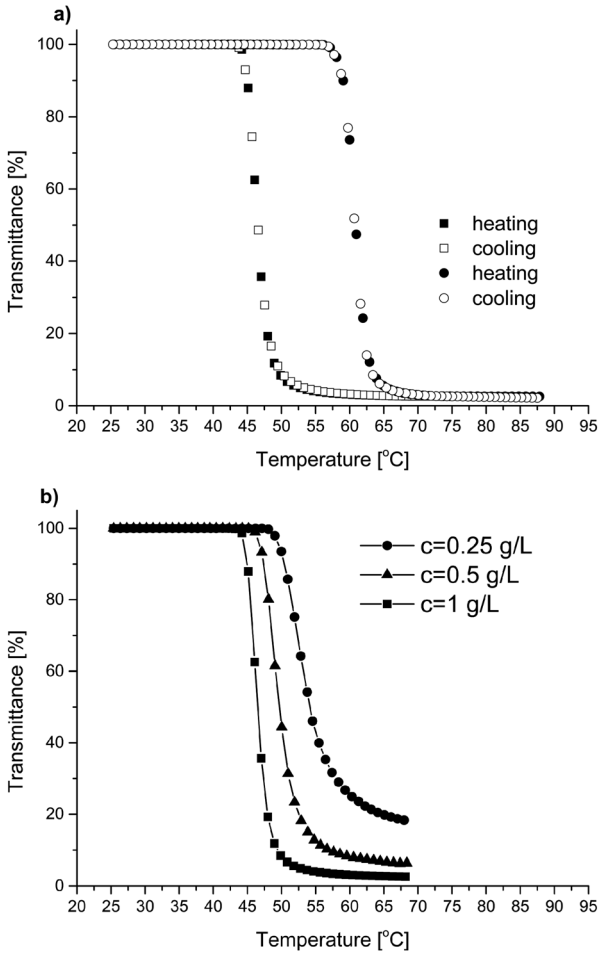

Fig. 6 (a) Transmittance *versus* temperature plots of P($HEMA_{70}$-*co*-$OEGMA_{30}$) (squares) and P($HEMA_{30}$-*co*-$OEGMA_{70}$) (circles) in an aqueous solution during the heating–cooling cycle, (b) transmittance *versus* temperature plot of various P($HEMA_{70}$-*co*-$OEGMA_{30}$) concentrations in aqueous solutions upon heating.

Open Access Article. Published on 11 December 2019. Downloaded on 2/20/2026 5:30:21 AM.
This article is licensed under a Creative Commons Attribution-NonCommercial 3.0 Unported Licence.

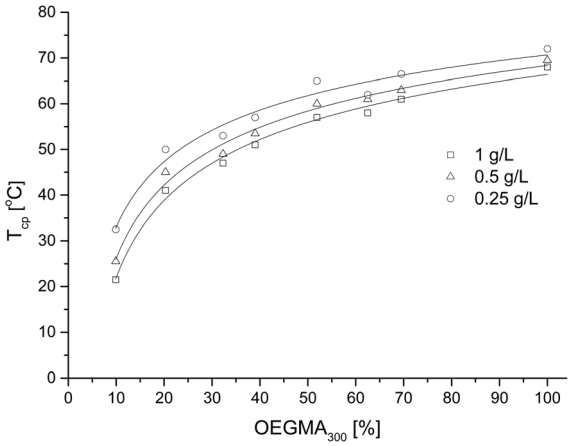

Fig. 7 Cloud point temperature of copolymer aqueous solutions with different concentrations *versus* mol percentage content of OEGMA. The lines drawn are logarithmic guides for the eye.

of concentration on T_{cp} for polymers based on monomers from the OEGMA group is usually observed.[15,62]

P(HEMA-*co*-OEGMA)s behavior in PBS solution

The behavior of the P(HEMA-*co*-OEGMA) copolymers and the P(OEGMA) homopolymer were also studied under conditions resembling physiological conditions, *i.e.*, in the phosphate buffer (PBS) solution at pH = 7.4 in heating/cooling cycles. The transmittance as a function of temperature is shown in Fig. 8a for the P($HEMA_{30}$-*co*-$OEGMA_{70}$) copolymer and in Fig. 8b for the P(OEGMA) homopolymer. The transmittance of both copolymer and homopolymer solutions first decreased to a minimum and later increased again. The measurements were carried out up to a temperature that significantly exceeded the temperature of the minimum transmittance. Then, the solution was cooled. The course of transmittance for the remaining P(HEMA-*co*-OEGMA) copolymers are shown in Fig. S4.†

The transition temperature has been determined as temperature value at a point of 50% decrease of transmittance during the heating cycle. The collected T_{cp} values are shown in Table S3.† The measured phase transition temperatures in PBS solution were 3.5 to 7 °C lower for all investigated (co)polymers than those in pure water solutions. This effect may be assigned to the action of the kosmotropic salts in the solution. In the case of pH 7.4 phosphate buffer, these are Na_2HPO_4 and KH_2PO_4 in the molar ratio of approximately 3.5 : 1. The kosmotropic salts are known to lower the interactions between macromolecules and water ("salting out" effect). It has been shown for poly(*N*-isopropylacrylamide) that the kosmotropic salts present in the solution lower the T_{cp}.[63,64] In PBS solutions, unlike in pure water, a significant difference between the transmittance curves when heating and when cooling the system was visible (Fig. 8). The observed transition was not fully reversible. The heating first caused a lowering of the transmittance, which increased again after a minimum was reached. After the measurement, a precipitated polymer resulting from macroscopic phase separation was found in the cuvette. This causes the

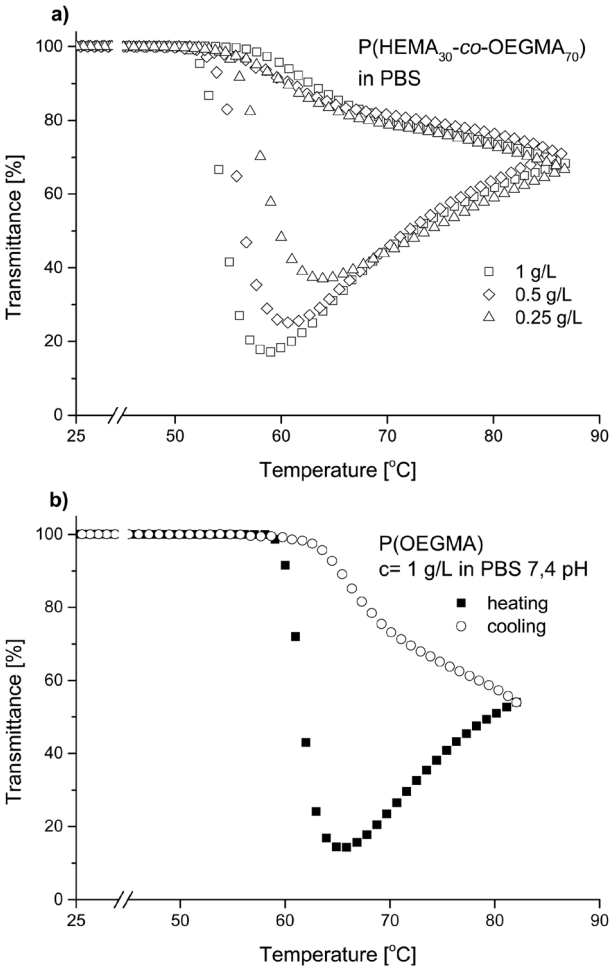

Fig. 8 Transmittance *versus* temperature plots of (a) a P($HEMA_{30}$-*co*-$OEGMA_{70}$) heating–cooling cycle in PBS solution of different concentrations, (b) a P(OEGMA) heating–cooling cycle in PBS solution.

concentration of dissolved polymer to be lower during cooling than at the beginning of the measurement and leads to transmittance increase compared to the heating mode.

Similar behavior was observed for all studied P(HEMA-*co*-OEGMA) copolymers at all concentrations (Fig. 8a) and also for the P(OEGMA) homopolymer (Fig. 8b).

As the precipitate is formed at temperatures well above T_{cp} also from the homopolymer P(OEGMA), which does not contain any OH groups, the deciding influence of these groups upon precipitate formation may be excluded. However, the hydrogen bond interaction most significantly influences the thermal stability of the gels. The copolymers containing 80% or 90% of HEMA units in the chain dissolved only when cooling the solutions to 4 °C. Copolymers with fewer HEMA units in the chain dissolved at room temperature upon stirring.

It was also searched for conditions enabling to reach reversible phase transitions in the buffer solutions. For this purpose, the solutions were heated only several degrees above the transition temperature and then cooled. Almost overlapping courses of the transmittance *versus* temperature when heating or when cooling the system were observed (Fig. 9). This seems to

Open Access Article. Published on 11 December 2019. Downloaded on 2/20/2026 5:30:21 AM.
This article is licensed under a Creative Commons Attribution-NonCommercial 3.0 Unported Licence.

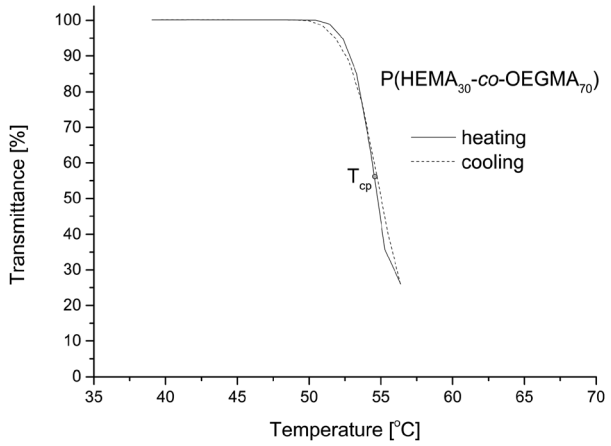

Fig. 9 Reversible phase transition for P($HEMA_{30}$-*co*-$OEGMA_{70}$) in a PBS solution.

confirm that in such a process, the aggregation happens to a much lesser extent making the process reversible.

At present, we are not able to offer any nonspeculative, well-founded explanation of the observed phenomena. Work towards this aim is in progress. However, it should be noted that a similar behavior was observed by Longenecker *et al.*[37] A copolymer of HEMA and sodium methacrylate was reported to precipitate from the 400 mM NaCl solution when the phase transition temperature was exceeded. Above the transition temperature, the precipitate formed in the solution was settled at the walls of the cuvette. After cooling, the precipitate did not dissolve, it was possible to it only after methanol was added to the solution. Additionally, an analysis of the data reported by Lavigueur *et al.*[65] concerning the behavior of the random copolymers of (diethylene glycol) acrylate and oligo(ethylene glycol) acrylate in PBS indicates the possibility of subsequent polymer aggregation after reaching maximum absorbance. A gradual decrease may be observed in the absorbance with increased temperature after T_{cp} was exceeded.

Conclusions

The synthetic strategy based upon ATRP led to thermoresponsive copolymers of HEMA and OEGMA monomers. Using a mixed DMSO/H_2O solvent system, copolymers of the aimed composition, low molar mass dispersity and random distribution of repeating units in the chain were obtained. Molar masses of P(HEMA-*co*-OEGMA) exceeded 30 kDa. The highest content of HEMA in the copolymer was 90 mol%, and the polymer remained water-soluble at room temperature. For the first time, copolymers with high amounts of HEMA in the chain and high molar mass that are still soluble in water close to room temperature and have LCST-type phase transition have been described. The thermoresponsiveness of the obtained copolymers was studied in water and in PBS solution (pH = 7.4). It was observed that in water, the transition temperature decreases with increasing content of HEMA units. HEMA acting in the chain as hydrophobic units. The studies of the concentration dependence of the aggregation of polymers indicate that at lower concentrations, the transition temperatures increase, and the transition becomes broader. Changing HEMA content in copolymers allows control over cloud point temperature in a wide range from 21.5 °C to 61.5 °C. This makes it possible to precisely adjust the temperature to the conditions necessary for future applications. This new copolymers, due to many reactive groups in the chain, open the route for more efficient drug carriers for controlled release.

Turbidity studies in PBS solutions have shown that the presence of salts (Na_2HPO_4 and KH_2PO_4) lowers the transition temperatures by *ca.* 7 °C at a polymer concentration of 1 g L^{-1}. The plots in the heating and cooling cycles do not overlap. Thermal aggregation of P(HEMA-*co*-OEGMA) in PBS results in precipitation of the polymers while heating above the temperature of the minimum transmittance, making the transition irreversible.

A detailed study of the thermal aggregation of P(HEMA-*co*-OEGMA)s will be shown later.

Conflicts of interest

There are no conflicts to declare.

Acknowledgements

This work was supported by state funds for the Centre of Polymer and Carbon Materials, Polish Academy of Sciences.

Notes and references

1 A. Utrata-Wesołek, B. Trzebicka and A. Dworak, *Polimery*, 2008, **10**, 717–724.
2 A. Utrata-Wesołek, B. Trzebicka and A. Dworak, *Polimery*, 2009, **5**, 334–341.
3 M. Wei, Y. Gao, X. Li and M. J. Serpe, *Polym. Chem.*, 2017, **8**, 127–143.
4 A. K. Teotia, H. Sami and A. Kumar, *Switch. Responsive Surfaces Mater. Biomed. Appl.*, 2015, pp. 3–43.
5 V. O. Aseyev, H. Tenhu and F. M. Winnik, in *Self Organized Nanostructures of Amphiphilic Block Copolymers II*, ed. A. H. E. Müller and O. Borisov, Springer Berlin Heidelberg, Berlin, Heidelberg, 2011, pp. 29–89.
6 J. Seuring and S. Agarwal, *Macromol. Rapid Commun.*, 2012, **33**, 1898–1920.
7 J. F. Lutz and A. Hoth, *Macromolecules*, 2006, **39**, 893–896.
8 K. Bebis, M. W. Jones, D. M. Haddleton and M. I. Gibson, *Polym. Chem.*, 2011, **2**, 975–982.
9 H. G. Schild, *Prog. Polym. Sci.*, 1992, **17**, 163–249.
10 M. Heskins and J. E. Guillet, *J. Macromol. Sci., Part A*, 1968, **2**, 1441–1455.
11 K. A. Dawson, A. V. Gorelov, E. G. Timoshenko, Y. A. Kuznetsov and A. Du Chesne, *Phys. A*, 1997, **244**, 68–80.
12 R. Hoogenboom, H. M. L. Thijs, M. J. H. C. Jochems, B. M. van Lankvelt, M. W. M. Fijten and U. S. Schubert, *Chem. Commun.*, 2008, 5758–5760.
13 C. Diehl and H. Schlaad, *Macromol. Biosci.*, 2009, **9**, 157–161.

Open Access Article. Published on 11 December 2019. Downloaded on 2/20/2026 5:30:21 AM. This article is licensed under a Creative Commons Attribution-NonCommercial 3.0 Unported Licence.

14 D. Szweda, R. Szweda, A. Dworak and B. Trzebicka, *Polimery*, 2017, **62**, 298.
15 B. Trzebicka, D. Szweda, S. Rangelov, A. Kowalczuk, B. Mendrek, A. Utrata-Wesołek and A. Dworak, *J. Polym. Sci., Part A: Polym. Chem.*, 2013, **51**, 614–623.
16 J.-F. Lutz, *Adv. Mater.*, 2011, **23**, 2237–2243.
17 S. Mura, J. Nicolas and P. Couvreur, *Nat. Mater.*, 2013, **12**, 991–1003.
18 A. Chilkoti, M. R. Dreher, D. E. Meyer and D. Raucher, *Adv. Drug Delivery Rev.*, 2002, **54**, 613–630.
19 K. Uhlig, E. Wischerhoff, J.-F. Lutz, A. Laschewsky, M. S. Jaeger, A. Lankenau and C. Duschl, *Soft Matter*, 2010, **6**, 4262–4267.
20 K. Uhlig, B. Boysen, A. Lankenau, M. Jaeger, E. Wischerhoff, J.-F. Lutz, A. Laschewsky and C. Duschl, *Biomicrofluidics*, 2012, **6**, 24129.
21 H. Kakwere and S. Perrier, *Polym. Chem.*, 2011, **2**, 270–288.
22 J. Montheard, M. Chatzopoulos and D. Chappard, *J. Macromol. Sci. Polymer Rev.*, 1992, 1–34.
23 L. S. Wan, H. Lei, Y. Ding, L. Fu, J. Li and Z. K. Xu, *J. Polym. Sci., Part A: Polym. Chem.*, 2009, **47**, 92–102.
24 J. Yang, P. Zhang, L. Tang, P. Sun, W. Liu, P. Sun, A. Zuo and D. Liang, *Biomaterials*, 2010, **31**, 144–155.
25 A. Gallardo, C. Parejo and J. San Román, *J. Controlled Release*, 2001, **71**, 127–140.
26 N. Agrawal, M. J. N. Chandrasekar and U. V. S. Sara, *PDA J. Pharm. Sci. Technol.*, 2010, **64**, 348–355.
27 L. Yuan, W. Chen, J. Li, J. Hu, J. Yan and D. Yang, *J. Polym. Sci., Part A: Polym. Chem.*, 2012, **50**, 4579–4588.
28 W. Chen, L. A. Shah, L. Yuan, M. Siddiq, J. Hu and D. Yang, *RSC Adv.*, 2015, **5**, 7559–7566.
29 T. Okano, T. Aoyagi, K. Kataoka, K. Abe, Y. Sakurai, M. Shimada and I. Shinohara, *J. Biomed. Mater. Res.*, 1986, **20**, 919–927.
30 J. Mokrý, J. Karbanová, J. Lukáš, V. Palečková and B. Dvořánková, *Biotechnol. Prog.*, 2000, **16**, 897–904.
31 L. M. Seifert and R. T. Greer, *J. Biomed. Mater. Res.*, 1985, **19**, 1043–1071.
32 R. P. Johnson, Y.-I. Jeong, E. Choi, C.-W. Chung, D. H. Kang, S.-O. Oh, H. Suh and I. Kim, *Adv. Funct. Mater.*, 2012, **22**, 1058–1068.
33 R. M. Trigo, M. D. Blanco, J. M. Teijón and R. Sastre, *Biomaterials*, 1994, **15**, 1181–1186.
34 X. Lou, S. Munro and S. Wang, *Biomaterials*, 2004, **25**, 5071–5080.
35 A. Gallardo, F. Fernández, P. Bermejo, M. Rebuelta, A. Cifuentes, J. C. Díez-Masa and J. San Román, *Biomaterials*, 2000, **21**, 915–921.
36 J. V. M. Weaver, I. Bannister, K. L. Robinson, X. Bories-Azeau, S. P. Armes, M. Smallridge and P. McKenna, *Macromolecules*, 2004, **37**, 2395–2403.
37 R. Longenecker, T. Mu, M. Hanna, N. A. D. Burke and H. D. H. Stöver, *Macromolecules*, 2011, **44**, 8962–8971.
38 Y. Miwa, H. Ishida, M. Tanaka and A. Mochizuki, *J. Biomater. Sci., Polym. Ed.*, 2010, **21**, 1911–1924.
39 L. Idowu and R. Hutchinson, *Polymers*, 2019, **11**, 487.
40 R. L. Teoh, K. B. Guice and Y.-L. Loo, *Macromolecules*, 2006, **39**, 8609–8615.
41 Z. Shen, K. Terao, Y. Maki, T. Dobashi, G. Ma and T. Yamamoto, *Colloid Polym. Sci.*, 2006, **284**, 1001–1007.
42 M. M. Fares and A. A. Othman, *J. Appl. Polym. Sci.*, 2008, **110**, 2815–2825.
43 W. Zhang, J. Li, W. Zhang, Z. Hu, X. J. Jiang, T. Ngai, P. C. Lo and G. Chen, *Polym. Chem.*, 2013, **4**, 782–788.
44 O. V. Khutoryanskaya, Z. a. Mayeva, G. a. Mun and V. V. Khutoryanskiy, *Society*, 2008, 3353–3361.
45 D. Lipowska-Kur, R. Szweda, B. Trzebicka and A. Dworak, *Eur. Polym. J.*, 2018, **109**, 391–401.
46 R. Szweda, B. Trzebicka, A. Dworak, Ł. Otulakowski, D. Kosowski, J. Hertlein, E. Haladjova, S. Rangelov and D. Szweda, *Biomacromolecules*, 2016, **17**, 2691–2700.
47 B. Trzebicka, R. Szweda, D. Kosowski, D. Szweda, Ł. Otulakowski, E. Haladjova and A. Dworak, *Prog. Polym. Sci.*, 2017, **68**, 35–76.
48 B. Trzebicka, B. Robak, R. Trzcinska, D. Szweda, P. Suder, J. Silberring and A. Dworak, *Eur. Polym. J.*, 2013, **49**, 499–509.
49 H. C. McCaig, E. Myers, N. S. Lewis and M. L. Roukes, *Nano Lett.*, 2014, **14**, 3728–3732.
50 T. Azzam and A. Eisenberg, *Angew. Chem., Int. Ed.*, 2006, **45**, 7443–7447.
51 B. Coto, J. M. Escola, I. Suárez and M. J. Caballero, *Polym. Test.*, 2007, **26**, 568–575.
52 G. Lligadas, S. Grama and V. Percec, *Biomacromolecules*, 2017, **18**, 2981–3008.
53 B. M. Rosen, X. Jiang, C. J. Wilson, N. H. Nguyen, M. J. Monteiro and V. Percec, *J. Polym. Sci., Part A: Polym. Chem.*, 2009, **47**, 5606–5628.
54 G. Lligadas and V. Percec, *J. Polym. Sci., Part A: Polym. Chem.*, 2008, **46**, 2745–2754.
55 J. Brandrup, E. H. Immergut, E. A. Grulke, A. Abe and D. R. Bloch, *Polymer handbook*, Wiley New York, 1999, vol. 89.
56 H. Fischer, *J. Polym. Sci., Part A: Polym. Chem.*, 1999, **37**, 1885–1901.
57 S. G. Roy, K. Bauri, S. Pal, A. Goswami, G. Madras and P. De, *Polym. Int.*, 2013, **62**, 463–473.
58 G. F. Estevez, O. V. Lizama, D. Z. Silva, L. Agüero and I. Katime, *Adv. Mater. Lett.*, 2013, **4**, 534–542.
59 D. Zhang, C. Macias and C. Ortiz, *Macromolecules*, 2005, **38**, 2530–2534.
60 F. Wu, X. Tang, L. Guo, K. Yang and Y. Cai, *Soft Matter*, 2013, **9**, 4036–4044.
61 M. Nardi, F. D'Acunzo, M. Clemente, G. Proietti and P. Gentili, *Polym. Chem.*, 2017, **8**, 4233–4245.
62 A. Dworak, D. Lipowska, D. Szweda, J. Suwinski, B. Trzebicka and R. Szweda, *Nanoscale*, 2015, **7**, 16823–16833.
63 Y. Zhang, S. Furyk, L. B. Sagle, Y. Cho, D. E. Bergbreiter and P. S. Cremer, *J. Phys. Chem. C*, 2007, **111**, 8916–8924.
64 Y. Zhang, S. Furyk, D. E. Bergbreiter and P. S. Cremer, *J. Am. Chem. Soc.*, 2005, **127**, 14505–14510.
65 C. Lavigueur, J. G. García, L. Hendriks, R. Hoogenboom, J. J. L. M. Cornelissen and R. J. M. Nolte, *Polym. Chem.*, 2011, **2**, 333–340.

 This journal is © The Royal Society of Chemistry 2019